Heliyon 6 (2020) e04545

Contents lists available at ScienceDirect

Heliyon

journal homepage: www.cell.com/heliyon

Research article

Interaction of different lipoprotein types with cholesterol at the air/water interface

Ryota Ninomiya, Cathy E. McNamee *

Shinshu University, Tokida 3-15-1, Ueda-shi, Nagano-ken 386-8567, Japan

ARTICLE INFO

Keywords:
Bioengineering
Biophysics
Physical chemistry
Thermodynamics
High density lipoproteins
Low density lipoproteins
Cholesterol
Langmuir monolayers
Fluorescence imaging

ABSTRACT

Cholesterol (Chol) interacts with lipoproteins, in order to be transported through the aqueous bloodstream. High density lipoproteins (HDL) and low density lipoproteins (LDL) transport cholesterol differently, a result that may be due to a difference in their interactions with cholesterol. Here, we investigated how the lipoprotein type affects the interaction with cholesterol by using a Langmuir trough and fluorescence microscope. We studied pure monolayers of 1) Chol, 2) LDL, and 3) HDL, and mixed monolayers of 1) Chol-LDL, and 2) Chol-HDL at air/water interfaces. Images of the Chol-LDL mixed monolayer showed many small sterol domains distributed in the non-sterol molecules (e.g. phospholids, proteins and lipids) of LDL. The sterol domains that were seen in the Chol-HDL mixed monolayer were larger in size but smaller in number than those seen in the Chol-LDL mixed monolayers. These images and the excess area, excess free energy, and free energy of mixing values obtained from the thermodynamic analysis of the surface pressure-area per molecule isotherms suggested that the cholesterol phase separated more from HDL than from LDL. Cholesterol was therefore concluded to interact with LDL better than with HDL. This more favorable interaction was explained by the presence of hydrophobic interactions between cholesterol and Apo-B, the major apoprotein of LDL.

1. Introduction

Cholesterol ("Chol") is a lipid that is an important component of cell membranes, which controls their permeability and fluidity [1]. It is also required in the synthesis of many molecules, such as bile acids and fat-soluble vitamins [2]. As the bloodstream is aqueous and lipids are mostly insoluble in water, a carrier protein is required to transport cholesterol. Lipoproteins allow lipids, including cholesterol, to be transported by forming particles with the lipids. The core of the particles consists of the hydrophobic lipids, and the exterior of the particles consist of the phospholipids and apoproteins found in the lipoproteins [3]. The low density lipoprotein ("LDL") is the major blood cholesterol carrier that transports cholesterol to the required site in the body [4]. The high density lipoproteins ("HDL") transports cholesterol back to the liver, where it is then either removed from the body or used by other tissues that synthesize hormones [5]. As HDL and LDL transports cholesterol differently, their interactions with cholesterol are expected to be different. It is important to understand the differences in the interaction of cholesterol with LDL and HDL, so as to better control the transport processes of cholesterol within the body.

The interaction of different components in a system is affected by the packing ability of the components in the system and the chemical and physical forces (e.g. van der Waals, hydrophobic attractions, electrostatic attractions and repulsions) in the system. Differences in the shapes of the chemical structure of the various components affect their packing ability and the types and magnitudes of the forces.

The interactions of LDL and HDL with cholesterol are expected to differ, as the composition of LDL and HDL are different. Both LDL and HDL contain lipids and apoproteins. The minor lipids found in LDL and HDL are cholesterol and triglycerides [6,7], and the major lipids are cholesteryl esters and phospholipids [7]. Although LDL and HDL contain the same lipid types, the ratio of these lipids is different (Table 1) [8,9]. Another difference between LDL and HDL are their main apoproteins. LDL contains apoprotein B (Apo-B) and HDL contains apoprotein A (Apo-A) [9]. Apo-B is a large hydrophobic protein, making it largely insoluble in water [8]. Apo-A has a much smaller molecular weight than Apo-B and is more soluble in water [10]. In addition, the apoproteins in the lipoprotein particles can change their conformation, when conditions such as the amount of lipid and the lipid composition change [9]. As the

* Corresponding author.
E-mail address: mcnamee@shinshu-u.ac.jp (C.E. McNamee).

https://doi.org/10.1016/j.heliyon.2020.e04545
Received 14 August 2018; Received in revised form 18 October 2018; Accepted 22 July 2020

physical properties of Apo-A and Apo-B are different, the way that Apo-A and Apo-B interact with cholesterol are expected to be different.

The ratio of HDL-cholesterol and LDL-cholesterol found in the bloodstream can be calculated to be 0.22 ± 0.11 and 0.62 ± 0.36 from the concentration of cholesterol, LDL and HDL in the bloodstream of healthy males [11]. The low ratio of cholesterol as to LDL compared to HDL also suggests that the interaction of cholesterol with LDL is different than with HDL.

The differences in the interactions of LDL and HDL with cholesterol can be studied by determining the differences in the way LDL and HDL mix with cholesterol. Monolayers of LDL from hen egg yolk have been studied at air/water interfaces using a Langmuir trough [12,13]. The LDL monolayer was shown to be stable, indicating that the physical properties of lipoproteins can be studied using a Langmuir trough. Cholesterol can also form a Langmuir monolayer at an air/water interface [14]. The differences in the interactions of LDL and HDL with cholesterol can therefore be studied by using a Langmuir trough to prepare mixed monolayers of cholesterol and LDL and mixed monolayers of cholesterol and HDL. Analysis of the surface pressure-area per molecule isotherms of mixed monolayers of lipoproteins and cholesterol composed of different lipoprotein:cholesterol ratios allows the excess area (ΔA^E), the excess free energy (ΔG^E), and the Gibbs free energy of mixing (ΔG^M) to be obtained. These thermodynamic properties give information about the ability of LDL and HDL to mix and therefore interact with cholesterol.

In this study, we aimed to determine the differences in the interaction of cholesterol with LDL and with HDL. This was achieved by using a Langmuir trough and fluorescence microscope to study how the physical properties of HDL monolayers and LDL monolayers at air/water interfaces changed in the presence of cholesterol. We investigated pure Langmuir monolayers of 1) Chol, 2) LDL, and 3) HDL, and mixed Langmuir monolayers of 1) Chol and LDL (Chol-LDL), and 2) Chol and HDL (Chol-HDL) at air/water interfaces. Langmuir isotherms of LDL films at air/water interfaces have previously been studied [12,13]. However, investigations of HDL monolayers at air/water interfaces are still lacking. A high ratio of cholesterol was used in the Chol-HDL mixed monolayers and Chol-LDL mixed monolayers, in order to identify the differences in the interactions of cholesterol with HDL and with LDL more easily. The surface pressure-area per molecule isotherms and fluorescence images were obtained for the different monolayers. These isotherms were also analysed to give the excess area, the excess free energy, and the Gibbs free energy of mixing of the mixed monolayers.

2. Experimental

2.1. Materials

The materials used were cholesterol (purity >99.5%, Wako, Japan), high density lipoprotein (human high density lipoprotein, Funakoshi, Japan), low density lipoprotein (human low density lipoprotein, Funakoshi, Japan), chloroform ("$CHCl_3$", purity >99%, Wako, Japan), methanol ("MeOH", purity >99.8%, Wako, Japan), ethanol ("EtOH", purity >99.5%, Wako, Japan), 25-[N-[(7-nitro-2-1,3-benzoxadiazol-4-yl) methyl]amino]-27-norcholesterol ("*25-NBD Cholesterol*", purity >99%, Funakoshi, Japan), and 1-Palmitoyl-2-{6-[(7-nitro-2-1,3-benzoxadiazol-4-yl)amino]hexanoyl}-sn-glycero-3-phosphocholine ("*16:0-06:0 NBD PC*", purity >99%, Funakoshi, Japan). All reagents were used as received. A water purification system (Direct-Q3 UV, Millipore, USA) was used to de-ionise the water to give a conductance of 18.2 MΩ cm^{-1} and a total organic content of <5 ppm.

In order to determine the spreading solution to prepare Langmuir monolayers of HDL and LDL monolayers, HDL and LDL were dissolved in a pure solvent or in a mixture of solvents composed of (1) 100% chloroform, (2) 100% ethanol, (3) 90% chloroform and 10% methanol, and (4) 85% chloroform and 15% methanol. All the spreading solvents prepared gave positive non-zero surface pressure values as the area values decreased, if the spreading solution was prepared on the same day as the isotherms were measured. The 85% chloroform and 15% methanol spreading solution gave the highest surface pressure, when the same area per molecule values obtained from the different spreading solution types were compared. Thus, the 85% chloroform and 15% methanol spreading solvent was concluded to best spread LDL and HDL at the air/water interface. In order to determine if the spreading solvent affected the components of HDL or LDL, the surface pressure-area isotherms that were measured on the same day as the spreading solution was prepared were compared to those measured two weeks after the spreading solution was prepared. The surface pressure-area isotherms did not change for the 85% chloroform and 15% methanol solution, if the spreading solution was prepared on the same day or two weeks before the isotherms were measured. This result suggested that HDL and LDL were not affected by this spreading solvent. In contrast, the 100% chloroform solution did not give a non-zero surface pressure-area isotherm, if the spreading solution was prepared two weeks before the isotherms were measured. Thus, the components in LDL and HDL were concluded to be affected by chloroform if the ratio of chloroform in the spreading solution was greater than 85%. The spreading solutions were prepared on the same day as the monolayers were measured. The concentration of the HDL, LDL and CHOL solutions was calculated using the weight of dry HDL, LDL, or Chol added to a known volume of the solvent.

The Chol-HDL and Chol-LDL spreading solutions were prepared by mixing a known volume of the Chol solution with a known volume of the HDL or LDL solutions to give solutions with a specific volume fraction of Chol, HDL, and LDL. The number fraction of Chol (X_{Chol}) was calculated using:

$$X_{Chol} = \frac{V_{f\_Chol} V_{spread} C_{Chol} N_A / M_{w\_Chol}}{V_{f\_Chol} V_{spread} C_{Chol} N_A / M_{w\_Chol} + (1 - V_{f\_Chol}) V_{spread} C_L N_A / M_{W\_L}} \quad (1)$$

Here, V_{f_Chol} is the volume faction of Chol in the spreading solution. V_{spread} is the volume of the Chol, HDL, LDL, mixed Chol-LDL, or mixed Chol-HDL solutions spread at the air/water interface. M_{w_Chol} and M_{w_L} are the molecular weights of cholesterol and the lipoprotein, respectively. In the case of HDL, the average of the molecular weight range of 1.75×10^5–3.60×10^5 $gmol^{-1}$ that was reported by the suppliers for HDL was used, i.e. 2.68×10^5 $gmol^{-1}$. In the case of LDL, the molecular weight of 2.30×10^6 $gmol^{-1}$ that was reported by the suppliers was used. C_{Chol}, C_L, and N_A are the concentrations of the pure Chol spreading solution, the pure lipoprotein spreading solutions, and Avagadro's number, respectively. The concentrations of the lipoprotein spreading solutions were calculated using the weight of the dried LDL or HDL added to a known volume of the spreading solvent and the molecular weight of the HDL or LDL. The number fractions of cholesterol in the Chol-HDL mixed monolayers and the Chol-LDL mixed monolayers used in this study are shown in Table 2.

The Chol and LDL or HDL phases in the mixed Chol-LDL or Chol-HDL monolayers were optically observed by adding *16:0-06:0 NBD PC* to the Chol, LDL, HDL, Chol-LDL or Chol-HDL solutions. The concentration of the fluorescence probe added to the spreading solutions was less than 1 mol%. Such low concentrations have little effect on the observed phase behaviours of the monolayers [15].

Table 1. The composition (percent dry weight) of plasma lipoproteins in LDL and HDL [8].

Composition	HDL	LDL
Triglycerides	8	8
Cholesteryl esters	20	40
Cholesterol	5	8
Phospholipids	30	22
Protein	37	22

2.2. Methods

2.2.1. Langmuir trough

The monolayers were prepared at room temperature (T = 298 K) by using a Langmuir-Blodgett Trough (Large microscopy Langmuir trough, Nima Technology Ltd, Coventry, UK) made from poly(tetrafluoroethylene) (PTFE). The trough had two PTFE barriers, which compressed around the centre of the trough (maximum surface area of trough = 290 cm^2). The surface pressure was measured using a Wilhelmy plate of wet filter paper (No.2 240mm, Toyo, Japan) that was suspended from a strain gauge (Nima PS4 surface pressure sensor, Nima Technology Ltd, Coventry, UK) [16].

The Langmuir trough was firstly cleaned with chloroform and then with ethanol. Water was then added and its surface cleaned by compressing the barriers to maximum and suctioning the water surface. The monolayers were prepared by spreading the solutions (Chol, HDL, LDL, Chol-HDL mixtures, or Chol-LDL mixtures) at the air/water interface with a 50 μL syringe (1705TLL, Hamilton, Switzerland). The complete evaporation of the spreading solution was ensured by waiting 10 min, before the monolayers were compressed with a speed of 115 cm^2min^{-1}. The surface pressure and area values were simultaneously recorded, giving the Π -area isotherms. The Π -area isotherm of each monolayer was repeated a minimum of three times in order to ensure reproducibility of the results. The area values were converted to area per molecule values (A) by calculating the number of molecules spread at the air/water interface from the volume spread at the interface, the concentrations of the Chol, HDL and LDL solutions used to prepare the spreading solutions, and the fractions of Chol, HDL and LDL in the spreading solutions.

The spreading solvents used to make monolayers were verified not to contain contaminates, as only zero Π values were measured, when the Π -area isotherm was measured after spreading solvents composed of only 85% chloroform and 15% methanol at the air/water interface.

2.2.2. Combined fluorescence microscope-Langmuir trough

A combined fluorescence microscope-Langmuir trough was used to image the monolayers at the air/water interface, when the monolayers were compressed to a certain surface pressure. The experimental set-up has been explained elsewhere [17]. The monolayers were prepared by firstly cleaning the Langmuir trough in the way described above. The fluorescent spreading solutions were then applied to the air/water interface using a 50 μL syringe (1705TLL, Hamilton, Switzerland), and 10 min was allowed for the solvent to evaporate. The monolayer was then compressed to the desired surface pressure. The surface pressure was maintained by using the surface pressure control option on the Langmuir trough, after which the image was taken. The fluorescence images of the monolayers were taken at the air/water interface in the order of low to high surface pressures. No bleaching of the fluorescent dye was observed. The $\prod$ –A isotherms of the monolayers in the presence and absence of the fluorescent dyes were comparable, indicating that the fluorescent dyes did not affect the interaction between Chol and LDL or HDL. Multiple images were taken using three lenses with different magnifications, so as to ensure that the images used in the manuscript were representative of the system. The size of the domains in the images was estimated by using the PhotoRuler Software.

3. Results

3.1. $\prod$ -A isotherms of the monolayers

3.1.1. Cholesterol monolayers

Figure 1 shows the $\prod$ -A isotherm of the cholesterol monolayer at the air/water interface. This isotherm resembles the $\prod$ -A isotherm of a cholesterol monolayer at the air/water interface reported by Savva and others [18], showing the reliability of the monolayer. High area per molecule values (A>70 $Å^2$) gave zero surface pressures, corresponding to a monolayer in a gaseous state. Compression of the monolayer from approx. 70 to 35 $Å^2$ caused the surface pressure to increase from 0 to approx. 20 mNm^{-1}. The non-linear region at low surface pressures has been assigned to a gas-liquid phase co-existence regime [18]. Further compression of the monolayer caused a steep increase of the surface pressure. The cholesterol monolayers are tightly packed to give a condensed monolayer in this region. The limiting area per molecule (A_0) of the Chol monolayer was determined to be approx. 37 ± 4 $Å^2$ (Table 2) by extrapolating the steepest $\prod$ -A region at small A to zero (see dashed line in Figure 1). This value is consistent with those reported in previous studies [19].

3.1.2. HDL or LDL monolayers

Figure 2A and B (curves 6) show the $\prod$ -A isotherms of the HDL monolayer and the LDL monolayer at air/water interfaces, respectively. The isotherms showed a shoulder, highlighted by the arrows in Figure 2, at A of approx. 5000 and 190000 $Å^2$ and at $\prod$ = 4 and 1.5 mNm^{-1} for the HDL and the LDL monolayers, respectively. Increasing the compression of the monolayers caused the slope of the isotherm to progressively increase. The value of A_0 obtained for the HDL and the LDL monolayer was 3758 ± 80 and 100330 ± 80 $Å^2$, respectively (Table 2). The hydrodynamic radius (R_H) of HDL and LDL has been reported to be 49–59 and 75–128 Å, respectively [20]. If we consider HDL and LDL to form globules at A_0, then we can estimate the radii of HDL and LDL by calculating $(A_0)^{0.5}$. Values of 61 ± 9 and 316 ± 9 Å were obtained for HDL and LDL, respectively. The $(A_0)^{0.5}$ value is comparable to the reported R_H value for HDL, suggesting that the components of HDL were closely packed as globules at the air/water interface at A_0. However, the $(A_0)^{0.5}$ value for LDL was higher than the reported R_H value for LDL, suggesting that the components of LDL did not form closely packed globules at the air/water interface at A_0.

The LDL from hen egg yolk is composed of neutral lipids, apoproteins, and phospholipids [21]. The surface pressure-area isotherm of a monolayer of LDL from hen egg yolk at an air/water interface can be found from studies by other groups to show transitions around $\prod$ = 6, 19, 41 and 54 mNm^{-1} [12,22]. These transitions were interpreted by comparing $\prod$-A isotherms obtained for the LDL monolayer with those obtained for a lipid monolayer, an apoprotein monolayer, and a phospholipid monolayer, and by imaging the monolayers with an Atomic Force Microscope (AFM) after the monolayers were transferred to substrates. The first transition of the LDL monolayer was explained by a change in the state of the monolayer from gaseous to liquid expanded. The second, third and forth transitions were attributed to the collapse of the neutral lipid, apoprotein, and phospholipid regions, respectively, in the LDL monolayer. AFM images of a LDL monolayer compressed to $\prod$ = 20 mNm^{-1} showed a multi-layer structure made up of patches of various heights and sizes [22]. This information indicated the squeezing out of the lipids from

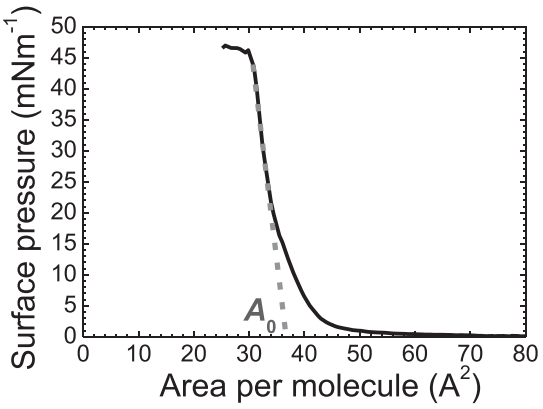

Figure 1. The surface pressure ($\prod$) - area per molecule (A) isotherms of the cholesterol monolayer. The dashed line highlights the area of closest packing (A_0).

Table 2. The limiting area per molecule (A_0) obtained for the Chol-HDL or Chol-LDL mixed monolayers with different molar fractions of cholesterol (X_{Chol}).

Mixed monolayers	X_{Chol}	A_0 (Å^2)
Chol-HDL	1.00	37 ± 4
	0.96 ± 0.01	540 ± 10
	0.90 ± 0.01	1000 ± 15
	0.80 ± 0.01	1240 ± 40
	0.51 ± 0.01	2540 ± 80
	0	3758 ± 80
Chol-LDL	1.00	37 ± 4
	0.98 ± 0.01	587 ± 40
	0.95 ± 0.01	654 ± 50
	0.89 ± 0.01	1211 ± 50
	0.67 ± 0.01	4170 ± 80
	0	100330 ± 80

the monolayer and the rearrangement of the apoprotein and phospholipids in the monolayer after the second transition. The transition at 54 mNm^{-1} corresponded to the collapse of the phospholipid region in the LDL monolayer.

The apoproteins in hen egg LDL have been reported to share a high identity and homology with the human apopliprotein B-100 [23], causing hen egg LDL to be considered as a potential replacement for human plasma LDL [24]. Due to this similarity between the hen egg LDL and human plasma LDL, the HDL monolayer and LDL monolayer made using human HDL and LDL in our study are expected to show similar properties to the monolayer of LDL from hen egg yolk at an air/water interface. Thus, information about the physical properties of the HDL and the LDL monolayers were obtained by comparing the $\prod$ -*A* isotherms of our HDL and LDL monolayers with those obtained by the monolayer of LDL from hen egg yolk at an air/water interface.

The shoulder in our HDL monolayer and our LDL monolayer is explained by the beginning of a gradual transition, involving a large area decrease consistent with a multi process of expulsion of hydrophobic segments and lipids, reorientation of the apolipoproteins conformation at the air/water interface and/or conformation change of proteins. Increasing the compression of the monolayer from the low-pressure regime towards the high-pressure regime resulted in a gradual increase in the surface pressure values. Lipid molecules in the monolayer of LDL from hen egg yolk case were reported to be squeezed out of the monolayer from the air/water interface towards the air phase at higher surface pressures [12,22]. Thus, the lipid molecules in our HDL and LDL monolayers are thought to be squeezed out of the monolayers from the air/water interface towards the air phase in this region. Alternatively, the lipids may have formed micelles, which then moved into the aqueous subphase. The A_0 was larger for the LDL monolayer than the HDL monolayer. The A_0 value of a monolayer is affected by the molecular weights of the components making up the monolayer. As the main apoprotein found in LDL (Apo-B) has a higher molecular weight than the apoprotein found in HDL (Apo-A), the higher A_0 value of the LDL monolayer than that of the HDL monolayer can be rationalized.

3.1.3. Mixed Chol-HDL or Chol-LDL monolayers

Information about the interaction of cholesterol with HDL or LDL can be obtained from the $\prod$-*A* isotherms of the Chol-HDL mixed monolayers (Figure 2A) and the Chol-LDL mixed monolayers (Figure 2B) at air/water interfaces. The $\prod$ -*A* isotherms of the Chol-HDL mixed monolayers (Figure 2A) and the Chol-LDL mixed monolayers (Figure 2B) showed different features, when the surface pressure was increased from a low-pressure regime towards the high-pressure regime. The Chol-HDL mixed monolayers with X_{Chol} = 0.80 and 0.51 (isotherm numbers 4 and 5 in Figure 2A) showed a wide shoulder at low surface pressures. The Chol-LDL mixed monolayers with X_{Chol} = 0.95, 0.89, and 0.67 (isotherm numbers 3, 4, and 5 in Figure 2B) showed a kink point at low surface pressures. The shoulder or kink is thought to indicate the onset of a phase boundary. These different features of the $\prod$ -*A* isotherms of the Chol-HDL mixed monolayers and the Chol-LDL mixed monolayers indicate that cholesterol mixed with HDL differently than with LDL. The values of A_0 of the Chol-HDL or Chol-LDL mixed monolayers were less than the A_0 of the pure HDL or LDL monolayers (Table 2). The ideal mean molecular areas of a mixed monolayer (A_{id}) can be calculated using [25]:

$$A_{id} = X_1 A_1 + X_2 A_2 \quad (2)$$

Here, X_1 and X_2 are the molar fractions of component 1 or 2 in the mixed monolayers. A_1 and A_2 are the area per molecules of components 1 and 2, respectively, in a pure monolayer of component 1 or component 2. Thus, the ideal values of A_0 of a mixed monolayer can be calculated via:

$$A_0 = X_{Chol} A_{0\_Chol} + (1 - X_{Chol}) A_{0\_Lip} \quad (3)$$

Here, X_{Chol} is the molar fractions of cholesterol in the mixed monolayers. A_{0_Chol} and A_{0_Lip} are the limiting area per molecule of cholesterol and the lipoprotein, respectively, in a pure monolayer of cholesterol or the lipoprotein. Cholesterol has a lower A_0 value than HDL and LDL, due to cholesterol having a much lower molecular weight than the apoproteins found in HDL and LDL. This fact combined with Eq. (3) shows that a decrease in the lipoprotein fraction in the mixed monolayer would

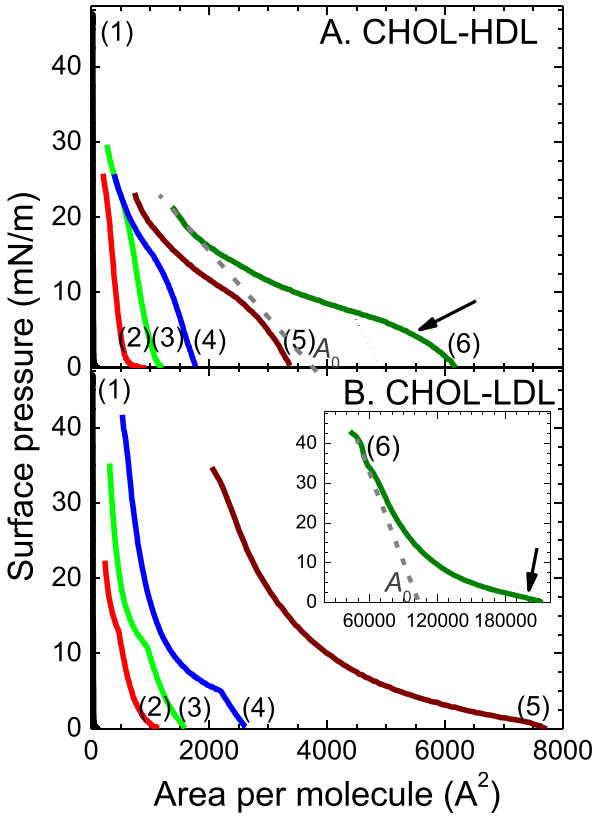

Figure 2. The surface pressure ($\prod$) - area per molecule (*A*) isotherms of the HDL monolayers and Chol-HDL mixed monolayers and the LDL monolayers and Chol-LDL mixed monolayers at the air/water interface for mixed monolayers with various number fractions of cholesterol (X_{Chol}). Panel A shows the Chol-HDL mixed monolayers with X_{Chol} = 1.00 (1), X_{Chol} = 0.96 (red line, 2),; X_{Chol} = 0.90 (3),X_{Chol} = 0.80 (4), X_{Chol} = 0.51 (5), and X_{Chol} = 0 (6). Panel B shows the Chol-LDL mixed monolayers with X_{Chol} = 1.00 (1), X_{Chol} = 0.98 (2), X_{Chol} = 0.95 (3), X_{Chol} = 0.89 (4), X_{Chol} = 0.67 (5). The insert in Figure 2B shows X_{Chol} = 0 (6). The arrows indicate the shoulder in the HDL and LDL isotherms. The dashed lines highlight the area of closest packing (A_0).

decrease the A_0 value of the Chol-HDL or Chol-LDL mixed monolayers. The LDL containing monolayers showed larger A_0 values than that of the HDL containing monolayers, when comparable number fractions of cholesterol were compared. This result is explained by the facts that the A_0 value of the pure LDL monolayer is higher than that of the pure HDL monolayer (see above) and that the A_0 value of the Chol-lipoprotein mixed monolayers depends on the A_0 value of the lipoprotein component (Eq. (3)).

3.2. Compression modulus of the monolayers

The compressibility (C_s) of the monolayers at the air/aqueous interfaces can be calculated from the $\prod$-A isotherms by using

$$C_s = -\frac{1}{A_\Pi}\left(\frac{dA}{d\Pi}\right) \quad (4)$$

Here, A_Π is the area per molecule at the specified surface pressure. The compression modulus (C_s^{-1}) of the monolayers is the reciprocal of the compressibility and can be used to describe the properties of the monolayers [26]. The C_s^{-1} value is zero for a clean air/water interface, and increases when surfactants are present at the air/water interface [27]. A larger C_s^{-1} value corresponds to a less compressible monolayer [28,29]. Liquid expanded, liquid-condensed and solid films are reported to have C_s^{-1} values between 12.5-50, 50–250, and above 250 mNm^{-1}, respectively [30,31]. Figure 3 shows the change in C_s^{-1} with the surface pressure for the Chol monolayer, the HDL monolayer, the LDL monolayer, the Chol-HDL mixed monolayers and the Chol-LDL mixed monolayers.

In the case of the Chol monolayer, the C_s^{-1} value increased with a surface pressure increase (Figure 3). The C_s^{-1} value for the Chol monolayer was $\leq$50 mNm^{-1} for surface pressures $\leq$ 5mNm^{-1}. These values correspond to a liquid expanded monolayer. A surface pressure increase to $\leq$20 mNm^{-1} gave a maximum C_s^{-1} value of approx. 200 mNm^{-1}. This value corresponds to a liquid-condensed monolayer. The C_s^{-1} value of a cholesterol monolayer compressed to Π = 20 mNm^{-1} at air/aqueous interfaces have ranged from 109 mNm^{-1} to values > 600 mNm^{-1} [18, 32–35]. The C_s^{-1} values are reported to change with the temperature and subphase pH of the system [32]. Other experimental conditions, such as the spreading solvent and compression speed, are also thought to influence the C_s^{-1} values [34]. The difference in our C_s^{-1} values from other groups is explained by a difference in the experimental conditions. The experimental conditions different to those used by other groups included the temperature [compared with ref. [32,33,35]], compression speed [compared with ref. [32–35]], spreading solvent [compared with ref. [32–34]], and subphase (pH, presence of salts, etc) [compared with ref. [32,36]],. The cholesterol monolayer gave larger C_s^{-1} values than the HDL or LDL monolayers. Thus, the cholesterol monolayer is considered to be more compressed than the lipoprotein monolayers.

In the case of the HDL monolayer, a maximum C_s^{-1} ($C_s^{-1}{}_{max}$) value was observed at Π = 1 mNm^{-1}. The C_s^{-1} values then decreased with a surface pressure increase. The addition of cholesterol to the HDL monolayer to give X_{chol} $\leq$0.90 increased the C_s^{-1} values. Values of X_{chol}>0.90 caused C_s^{-1} to decrease. A maximum in the C_s^{-1} values was observed in the Chol-HDL mixed monolayers, when C_s^{-1} was plotted against the surface pressure. The position of $C_s^{-1}{}_{max}$ shifted to higher surface pressure values as X_{chol} was increased.

In the case of the LDL monolayer, the C_s^{-1} values increased with a surface pressure increase. The C_s^{-1} values of the LDL monolayer were lower than those of the HDL monolayer at all surface pressures. These results indicate that the LDL monolayer was more compressible than the HDL monolayer. The addition of cholesterol to the LDL monolayer to give $X_{chol}\leq$0.95 caused C_s^{-1} to increase. Further increase in the X_{chol} values reduced the C_s^{-1} values. No maximum was seen in the C_s^{-1} – surface pressure plots for X_{chol} = 0 and 0.67. However, the Chol-LDL mixed monolayers with X_{chol} $\geq$0.89 gave C_s^{-1} - surface pressure plots that showed a maximum ($C_s^{-1}{}_{max}$). The position of $C_s^{-1}{}_{max}$ shifted to higher surface pressure values as X_{chol} was increased.

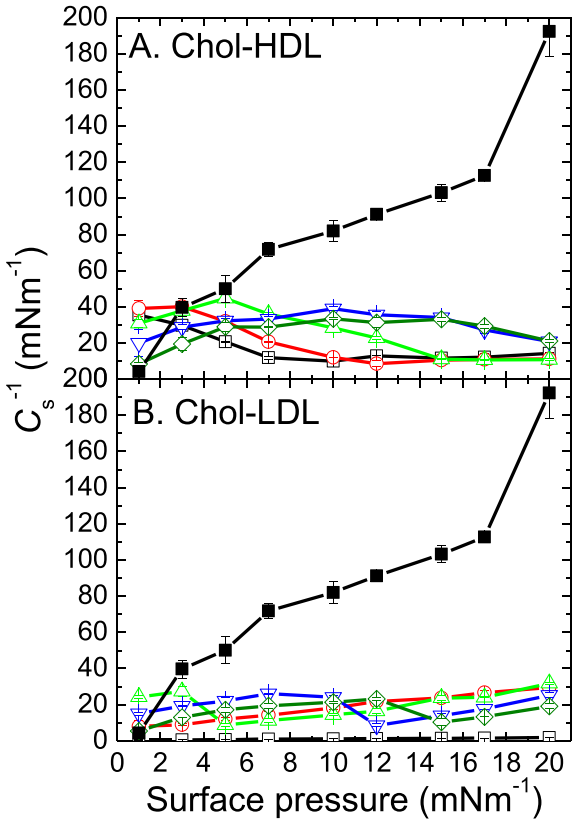

Figure 3. The change in compression modulus (C_s^{-1}) [1] with the surface pressure for the Chol-HDL mixed monolayers and the Chol-LDL mixed monolayers for monolayers with different number fractions of cholesterol (X_{Chol}). Panel A shows Chol-HDL mixed monolayers with X_{Chol} = 0 (□),X_{Chol} = 0.51 (○), X_{Chol} = 0.80 (Δ), X_{Chol} = 0.90 (▽), X_{Chol} = 0.96 (◇), and X_{Chol} = 1.0 (■). Panel B shows Chol-LDL mixed monolayers with X_{Chol} = 0 (□),X_{Chol} = 0.67 (○), X_{Chol} = 0.89 (Δ), X_{Chol} = 0.95 (▽), X_{Chol} = 0.98 (◇), and X_{Chol} = 1.0 (■).

The addition of cholesterol to the HDL or LDL monolayers tended to cause the $C_s^{-1}{}_{max}$ values to shift towards higher surface pressure values as the X_{Chol} value in the Chol-HDL or Chol-LDL mixed monolayers was increased. A dramatic drop in the C_s^{-1} values with a surface pressure increase has been reported to reflect discontinuities in the lateral packing at phase boundaries [28]. Thus, the presence of a maximum in the C_s^{-1} values for the cholesterol-lipoprotein mixed monolayer suggests that cholesterol did not ideally mix with the lipoproteins and that domains formed in the mixed monolayers. The difference in the shape and magnitude of the C_s^{-1} - surface pressures curves suggest a difference in the domain formation in the Chol-HDL mixed monolayers and the Chol-LDL mixed monolayers.

3.3. Fluorescence images of the monolayers

Further information about how the addition of cholesterol to the HDL or LDL monolayers affects the properties of the monolayers was obtained by using a fluorescence microscope and by adding the *25-NBD Cholesterol* fluorescent probe or the *16:0-06:0 NBD PC* fluorescent probe to the monolayers. The *25-NBD Cholesterol* probe partitions with the molecules with structures similar to sterol molecules in the monolayers, such as cholesterol and cholesteryl esters. It dissolves in the sterol domains with disordered phases, as the structure of the *25-NBD Cholesterol* fluorescent probe is more bulky than the sterol molecules. The *16:0-06:0 NBD PC*

fluorescent probe partitions with the molecules with structures similar to the phospholipid found in liposomes, such as 1-oleoyl-2-palmitoyl-sn-glycero-3-phosphocholine [24,28]. It dissolves in the phospholipid domains with disordered phases (LE phase) and highlights those domains, as the structure of the *16:0-06:0 NBD PC* fluorescent probe is more bulky than the phospholipid molecules.

3.3.1. Cholesterol monolayers

The cholesterol monolayer at an air/water interface could be imaged when the monolayer contained the *25-NBD Cholesterol* fluorescent probe. Figure 4M–P show the fluorescence images of a cholesterol monolayer containing the *25-NBD Cholesterol* fluorescent probe at an air/water interface, when the monolayer was compressed to 5, 10, 15, and 20 mNm^{-1}, respectively. The bright regions are assigned to LE phases. The dark regions are assigned to areas of LC phase or areas of a bare water surface not covered by cholesterol molecules. An increase in the dark areas with a surface pressure increase indicates that the dark area is due to cholesterol domains with ordered phases (LC phases). Bright areas were observed in the images at all the studied surface pressures. The average size of these domains at $\prod = 5\ mNm^{-1}$ was estimated to be 6.5 ± 1.3 μm. The size of these bright areas tended to decrease and become denser with a surface pressure increase of up to 20 mNm^{-1}. Brewster angle microscopic studies made by other groups have shown that cholesterol molecules fuse to give microscopic domains that are loosely packed at the air/water interface for surface pressures corresponding to a gas-liquid phase co-existence regime [37]. The $\prod$-*A* isotherm of cholesterol from above suggested a gas-liquid phase co-existence regime for $\prod \leq 20\ mNm^{-1}$. Thus, these bright areas are attributed to the microscopic domains of cholesterol in the liquid phase (LE phase).

3.3.2. Effect of cholesterol on the HDL or LDL monolayers

The fluorescence images of the Chol-HDL mixed monolayers containing the *25-NBD Cholesterol* fluorescent probe and the *16:0-06:0 NBD PC* fluorescent probe are shown in Figures 4 and 5, respectively. The bright regions in the images obtained using the *NBD Cholesterol* fluorescent probe were assigned to sterol domains in the LE phases. The bright regions obtained using the *16:0-06:0 NBD PC* probe were assigned to phospholipid domains with disordered phases. The dark regions seen in the images obtained using the *NBD Cholesterol* fluorescent probe correlate with the bright regions in images obtained using the *16:0-06:0 NBD PC* probe, showing that our assignment of the sterol domains is acceptable.

The HDL monolayer ($X_{Chol} = 0$) is seen from Figures 4 and 5 to be composed of small circular domains distributed throughout the rest of the monolayer. The average size of these domains at $\prod = 5\ mNm^{-1}$ was estimated to be 6.9 ± 2.5 μm. The sterol domains are assigned to the sterol molecules that are found in HDL. Lipoprotein particles have been reported to break at the air/water interface and allow the liberation of the free lipids from the lipoprotein core [30]. The images of the HDL monolayer are therefore interpreted to show domains of sterol molecules distributed throughout the rest of the monolayer, assigned to phospholipid and protein molecules. An increase in the surface pressure did not significantly change the area of the phospholipid and protein molecules, seen as the white regions observed in the images taken using the *16:0-06:0 NBD PC* fluorescent probe (Figure 5A–D). Thus, the phospholipid and protein molecules are concluded to be in a disordered packing for surface pressures $\leq 20\ mNm^{-1}$.

The addition of cholesterol to a pure HDL monolayer to give Chol-HDL mixed monolayers is seen in Figures 4 and 5 showing the forma-

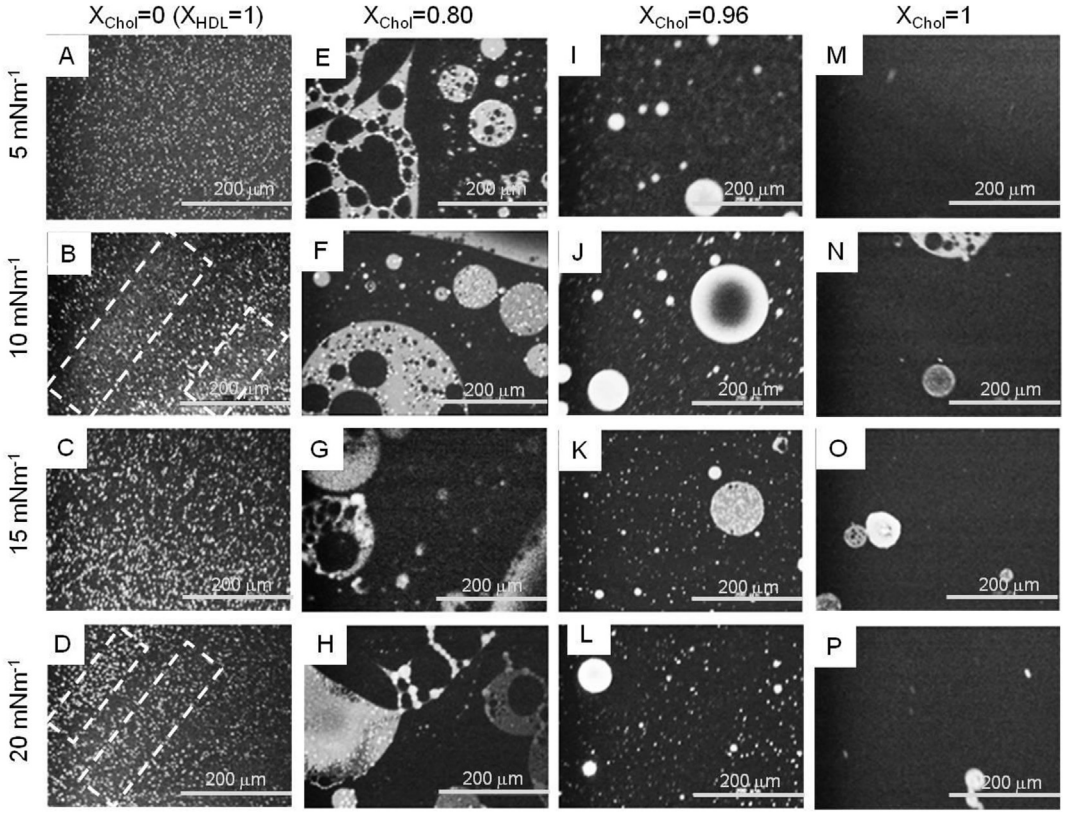

Figure 4. Typical fluorescence images of Chol-HDL mixed monolayers monolayers with different number fractions of cholesterol (X_{Chol}) compressed to $\prod$ = 5, 10, 15, and 20 mNm^{-1}, when imaged using NBD cholesterol as the fluorescent probe. A–D: $X_{Chol} = 0$; E–H: $X_{Chol} = 0.8$; I–L: $X_{Chol} = 0.96$, and M–P: $X_{Chol} = 1.0$. A, E, I, M: $\prod = 5\ mNm^{-1}$; B, F, J, N: $\prod = 10\ mNm^{-1}$; C, G, K, O: $\prod = 5\ mNm^{-1}$; and D, H, L, P: $\prod = 20\ mNm^{-1}$. The dashed white lines highlight the stripe-like patterns in the monolayers. The scale bar is 200 μm.

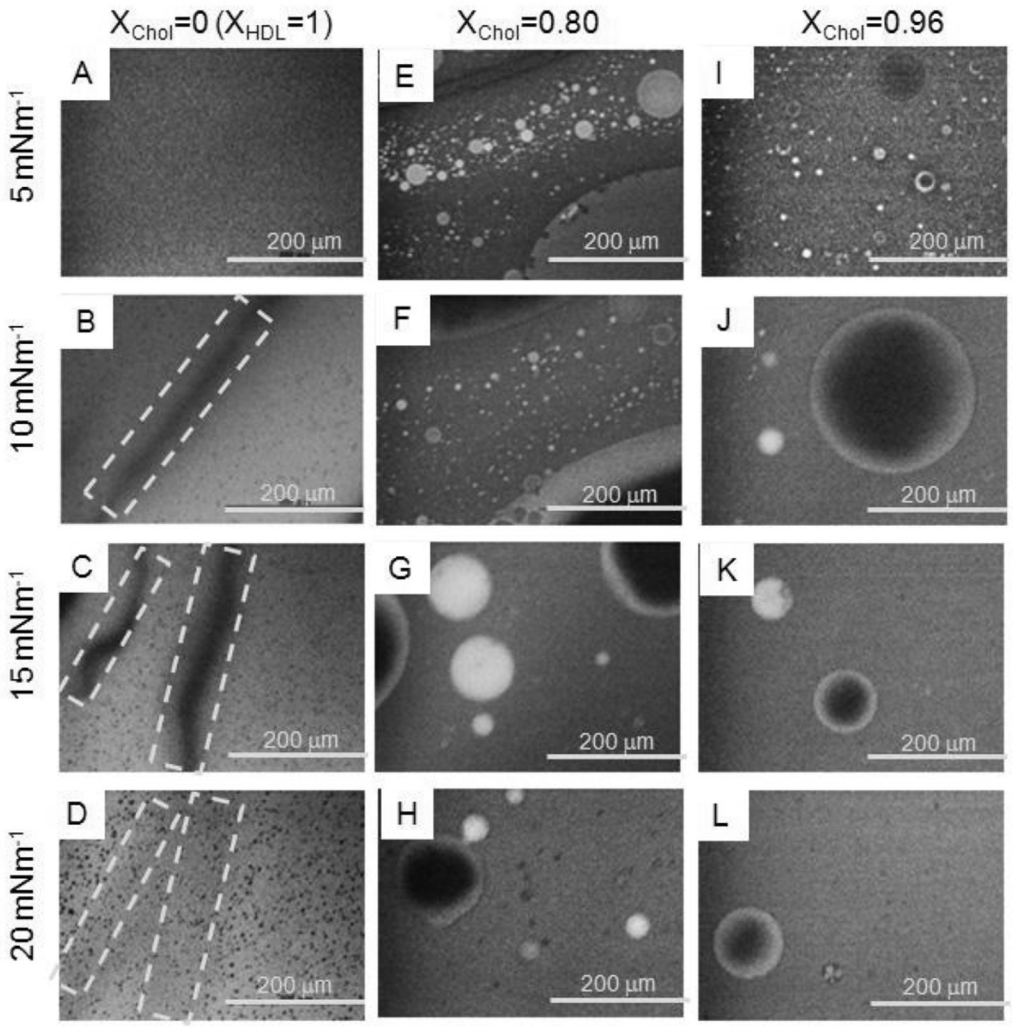

Figure 5. Typical fluorescence images of Chol-HDL mixed monolayers monolayers with different number fractions of cholesterol (X_{Chol}) compressed to $\prod$ = 5, 10, 15, and 20 mNm^{-1}, when imaged using *16:0-06:0 NBD PC* as the fluorescent probe. A–D: X_{Chol} = 0; E–H: X_{Chol} = 0.8; and I–L: X_{Chol} = 0.96. A, E, I: $\prod$ = 5 mNm^{-1}; B, F, J: $\prod$ = 10 mNm^{-1}; C, G, K: $\prod$ = 5 mNm^{-1}; and D, H, L: $\prod$ = 20 mNm^{-1}. The dashed white lines highlight the stripe-like patterns in the monolayers. The scale bar is 200 μm.

tion of sterol domains and domains of phospholipids and proteins. The $\prod$ -*A* isotherms of Figure 2A indicated that the molecules in the Chol-HDL mixed monolayers were in a liquid expanded region at < *Π* = approx. 20 mNm^{-1}. Thus, the domains of phospholipids and proteins were concluded to be loosely packed. In general, the addition of cholesterol to a pure HDL monolayer to give Chol-HDL mixed monolayers with X_{Chol} = 0.8 and 0.96 increased the size of the sterol domains for all the surface pressures. Domains with sizes >80 and 70 μm were observed for the Chol-HDL mixed monolayers with X_{Cho} = 0.8 and 0.96, respectively, when the surface pressure was 5 and 20 mNm^{-1}. As the sizes of the sterol domains for the X_{Chol} = 0.8 and 0.96 monolayers were larger than those observed in the pure HDL monolayer, these sterol domains were concluded to contain the cholesterol molecules that were added to the HDL monolayer. Increasing the surface pressure in the Chol-HDL mixed monolayers tended to decrease the holes in the domains, i.e. the packing density of the molecules in the domains increased with a surface pressure increase.

The fluorescence images of the Chol-LDL mixed monolayers containing the *25-NBD Cholesterol* fluorescent probe and the *16:0-06:0 NBD PC* fluorescent probe are shown in Figures 6 and 7 respectively. The bright regions in the images obtained using the *NBD Cholesterol* fluorescent probe were assigned to sterol domains in the LE phases. The bright regions obtained using the *16:0-06:0 NBD PC* probe were assigned to phospholipid domains with disordered phases.

The LDL monolayer (X_{Chol} = 0) as seen from Figures 6 and 7 is composed of small circular domains distributed throughout the rest of the monolayer. The average size of these domains at $\prod$ = 5 mNm^{-1} was estimated to be 14 ± 7 μm. These small domains were assigned to the sterol molecules found in LDL, and the other areas were assigned to phospholipid and protein molecules. The sizes of the domains in the LDL monolayer were larger than those found in the HDL monolayer. This result is explained by the fact that the apoprotein in LDL is larger than that found in HDL. The area of the white regions assigned to phospholipid and protein molecules in the LDL monolayer images obtained using the *16:0-06:0 NBD PC* probe (Figure 7A–D) did not appear to significantly change with a surface pressure increase to 10 mNm^{-1} and higher. The $\prod$ -*A* isotherms of Figure 2B indicated that the molecules in the LDL monolayer were still in a liquid expanded region at this surface pressure. Thus, the packing of the phospholipid and protein molecules in the LDL monolayer is thought to remain disordered for surface pressures up to 20 mN/m.

The addition of cholesterol to a pure LDL monolayer to give Chol-LDL mixed monolayers is shown in Figures 6 and 7. Small sterol domains are still observed after the addition of cholesterol. Increasing the surface pressure in the Chol-LDL mixed monolayers tended to increase the packing density of these sterol domains.

Stripe-like patterns were observed in the fluorescence images of the HDL and LDL monolayers for $\prod$ ≥10 (Figures 4B and D, 5B–D, 6C and D,

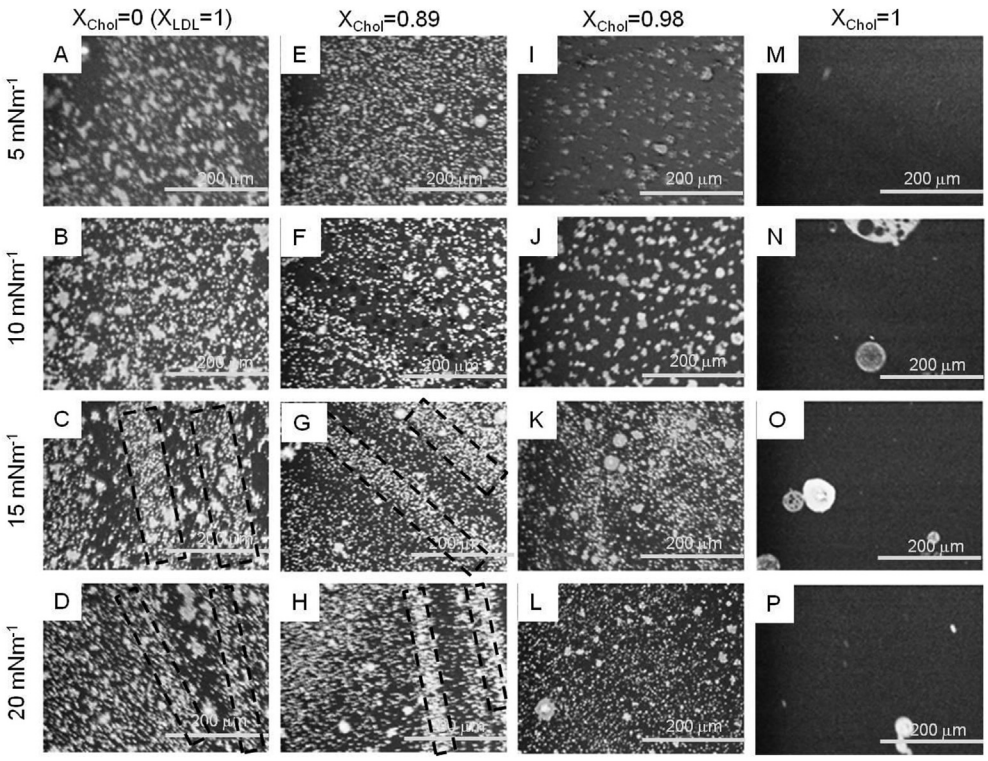

Figure 6. Typical fluorescence images of Chol-LDL mixed monolayers monolayers with different number fractions of cholesterol (X_{Chol}) compressed to $\prod$ = 5, 10, 15, and 20 mNm^{-1}, when imaged using NBD cholesterol as the fluorescent probe. A–D: X_{Chol} = 0; E–H: X_{Chol} = 0.89; I–L: X_{Chol} = 0.98; and M–P: X_{Chol} = 1.0. A, E, I, M: $\prod$ = 5 mNm^{-1}; B, F, J, N: $\prod$ = 10 mNm^{-1}; C, G, K, O: $\prod$ = 5 mNm^{-1}; and D, H, L, P: $\prod$ = 20 mNm^{-1}. The dashed black lines highlight the stripe-like patterns in the monolayers. The scale bar is 200 μm.

7B and C) and in the Chol-LDL mixed monolayer with $X_{Chol} = 0.89$ for $\Pi \geq 10$ mNm^{-1} (Figure 6G and H). These stripes are highlighted by the dashed boxes in the fluorescence images. In the case of the pure HDL or LDL monolayers, the monolayers show phase separated domains, explained by the break-up of islands of the aggregated lipoprotein. These phase separated domains may form the stripe-like pattern in the monolayer at increased surface pressures, due to the compression of the monolayer. The addition of cholesterol tended to decrease the formation of these stripes, indicating that the presence of cholesterol affects the domains formed by HDL and LDL.

Comparison of the fluorescence images of the Chol-LDL mixed monolayers and the Chol-HDL mixed monolayers showed that the sizes of the sterol domains were smaller for the Chol-LDL mixed monolayers than the Chol-HDL mixed monolayers. The sizes of the sterol domains in the Chol-LDL mixed monolayer were also more constant than those in the Chol-HDL mixed monolayers. The number of sterol domains, however, was higher for the Chol-LDL mixed monolayers than for the Chol-HDL mixed monolayers. These differences are explained by a difference in the interactions of cholesterol with the components of LDL compared to that with the components of HDL. The large size and low number of sterol domains found in the Chol-HDL mixed monolayers could be explained, if the cholesterol phase is separating stronger from the non-sterol components of HDL than those of LDL. The small size and high number of sterol domains found in the Chol-LDL mixed monolayers could be explained, if the cholesterol phase can interact with the components of LDL, e.g. via an attractive molecular interaction.

3.4. Thermodynamics of the monolayers

Information about the mixing of Chol with HDL or with LDL was obtained by measuring the area per molecule values of the mixed films from the isotherms of Figure 2. The excess area (ΔA^E) shows whether the mixing is ideal or non-ideal. It is calculated using [25]:

$$\Delta A^E = A_{1,2} - A_{id} \quad (5)$$

$A_{1,2}$ are the experimentally determined area per molecule of the mixed monolayers. A non-zero ΔA^E value indicates that the mixing of the two components in the mixed monolayer is non-ideal [38]. A zero ΔA^E value indicates that the mixing is ideal, where an ideal monolayer is one that is completely mixed (homogeneous mixing) or completely immiscible (phase separated).

Figure 8 shows the effect of the surface pressure of the monolayer and the fraction of Chol in the Chol-HDL or Chol-LDL mixed monolayers on ΔA^E. Both the Chol-HDL mixed monolayer and the Chol-LDL mixed monolayer gave non-zero ΔA^E values, indicating non-ideal mixing. However, the Chol-LDL mixed monolayers case gave negative ΔA^E values, while the Chol-HDL mixed monolayers gave positive ΔA^E values. A negative deviation shows a condensation effect, while positive deviations show an expanded film [38].

Information about the molecular interactions in the mixed monolayers was obtained from the excess Gibbs free energy (ΔG^E), which is calculated via [39]:

$$\Delta G^E = \int_0^{\Pi} (A_{1,2} - A_{id}) d\Pi \quad (6)$$

Here, $A_{1,2}$ is the area per molecule of component 1 in a mixed monolayer of components 1 and 2, i.e. the experimentally measured area per molecule of the mixed film. Positive ΔG^E values indicate repulsive molecular interactions between the monolayer components, while negative ΔG^E values indicate the existence of attractive molecular interactions between two components in the mixed monolayer [39].

Figure 9 shows the change in ΔG^E with the fraction of Chol in the Chol-HDL or Chol-LDL mixed monolayers and the surface pressure of the monolayer. In the case of the Chol-HDL mixed monolayers, positive ΔG^E values were observed. This result indicated the presence of repulsive molecular interactions between the monolayer components. The positive ΔG^E values increased, when the surface pressure was increased from 5 to 15 mNm^{-1}. Increasing the surface pressure from 15 to 20 mNm^{-1} tended to decrease the ΔG^E values. In the case of the Chol-LDL mixed monolayers, negative ΔG^E values were observed. This result indicated the presence of attractive molecular interactions between the monolayer

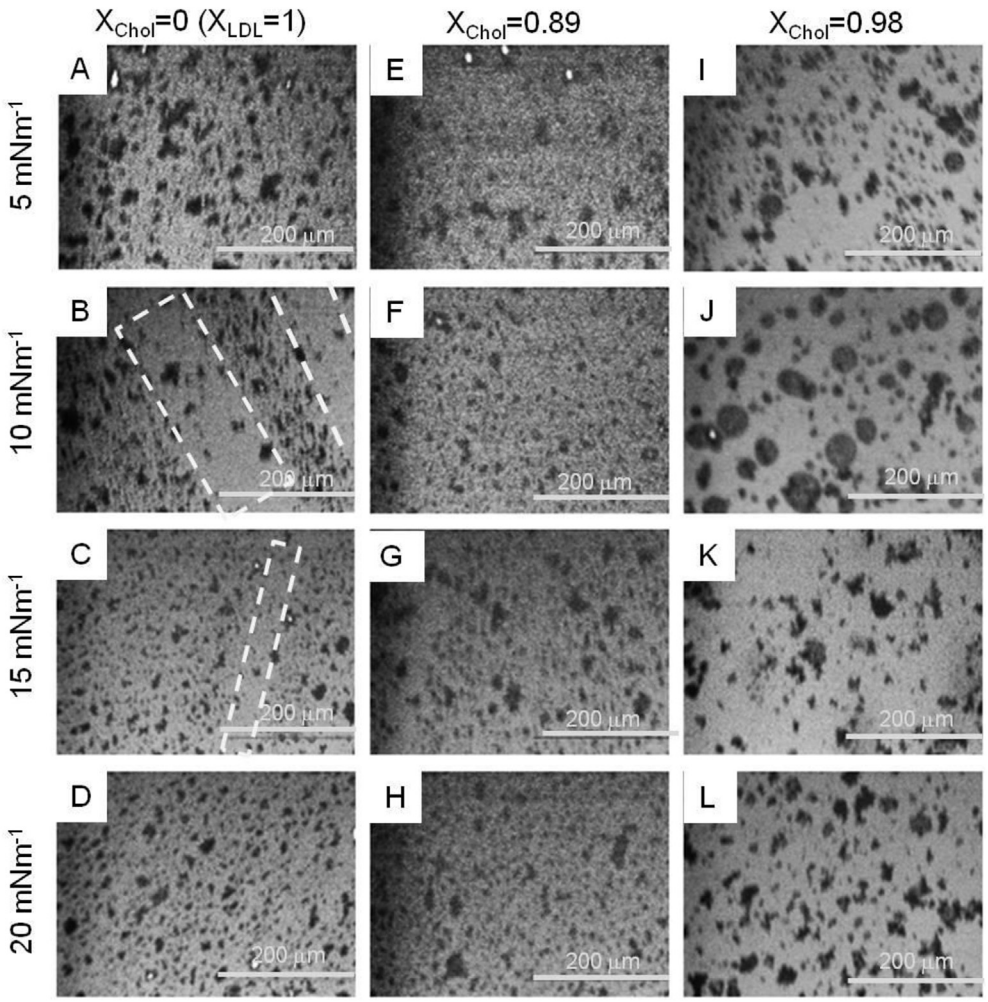

Figure 7. Typical fluorescence images of Chol-LDL mixed monolayers monolayers with different number fractions of cholesterol (X_{Chol}) compressed to $\prod$ = 5, 10, 15, and 20 mNm^{-1}, when imaged using *16:0-06:0 NBD PC* as the fluorescent probe. A–D: X_{Chol} = 0; E–H: X_{Chol} = 0.89; and I–L: X_{Chol} = 0.98. A, E, I: $\prod$ = 5 mNm^{-1}; B, F, J: $\prod$ = 10 mNm^{-1}; C, G, K: $\prod$ = 5 mNm^{-1}; and D, H, L: $\prod$ = 20 mNm^{-1}. The dashed white lines highlight the stripe-like patterns in the monolayers. The scale bar is 200 μm.

components. The ΔG^E values became more negative as the surface pressure was increased from 5 to 20 mNm^{-1}. The facts that the Chol-LDL mixed monolayer gave negative ΔG^E values and the Chol-HDL mixed monolayer gave positive ΔG^E values suggest cholesterol can pack with LDL more efficiently than with HDL. This result is also supported by the fluorescence images of the mixed monolayers, which showed that larger sterol domains were obtained for the Chol-HDL mixed monolayer than the Chol-LDL monolayer. The larger sterol domain sizes suggest that the cholesterol phase separates from the non-sterol components of HDL more than from the non-sterol components of LDL.

The increase in the positive ΔG^E values with a surface pressure increase for the Chol-HDL mixed monolayers can be explained by an increase in the repulsive molecular interactions between the monolayer components with a surface pressure increase. The $\prod$-*A* isotherms showed that a surface pressure increase decreased the surface area available for the Chol-HDL mixed monolayers. This would result in a decrease of the molecular packing density. The conformation of the apoproteins in the monolayers could change, e.g., form loops, and the molecules in the monolayer would overlap more as the molecules in the monolayers are forced to pack tighter. These geometric constraints of the components in the mixed monolayer would cause steric repulsions in the mixed monolayer that could increase the ΔG^E values. The decrease in the magnitude of ΔG^E with a surface pressure increase from 15 to 20 mNm^{-1} for the Chol-HDL mixed monolayers indicates a decrease in the repulsive molecular interactions between the monolayer components. This decrease can be explained by a reduced steric repulsion due to a more favorable packing of the molecules in the mixed monolayer, which may result from (1) the squeezing out of the neutral lipids in the Chol-HDL mixed monolayers at higher surface pressures or (2) the decrease in the size and number of the holes in the sterol domains that accompanied an surface pressure increase from 15 to 20 mN/m (see fluorescence images shown in Figure 4G and H).

The fact that the ΔG^E values were negative for all the surface pressures measured for the Chol-LDL mixed monolayers indicates the presence of attractive molecular interactions at all surface pressures. Increasing the surface pressure increases the packing density, which would decrease the separation distance between the components and thereby increase the magnitude of interaction by the attractive forces. This could have caused the negative ΔG^E values to become more negative as the surface pressure was increased. The increase in the magnitude of the negative ΔG^E values from 15 to 20 mNm^{-1} is thought to be related to the squeezing out of the neutral lipids at higher surface pressures, which would decrease the steric repulsions between the components in the mixed monolayer.

Information about the stability of the mixed monolayers was obtained from the Gibbs free energy of mixing (ΔG^M), which can be calculated using [40].

$$\Delta G^M = \Delta G^{id} + \Delta G^E \quad (7)$$

Here, ΔG^{id} and ΔG^E are the change of the ideal Gibbs free energy and the excess Gibbs free energy, respectively. ΔG^{id} is calculated via [40]:

$$\Delta G^{id} = RT(X_1 \ln X_1 - X_2 \ln X_2) \quad (8)$$

Here, R and T are the gas constant and the absolute temperature, respectively.

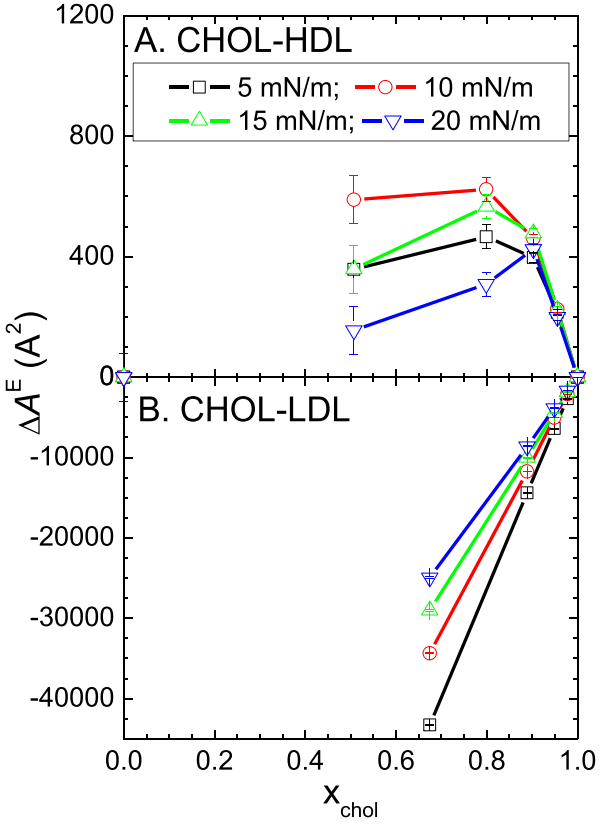

Figure 8. The excess area (ΔA^E) of Chol-HDL mixed monolayers (panel A) and Chol-LDL mixed monolayers (panel B) as a function of the molar fraction of cholesterol (X_{Chol}) in the mixed monolayers for different surface pressures (∏).

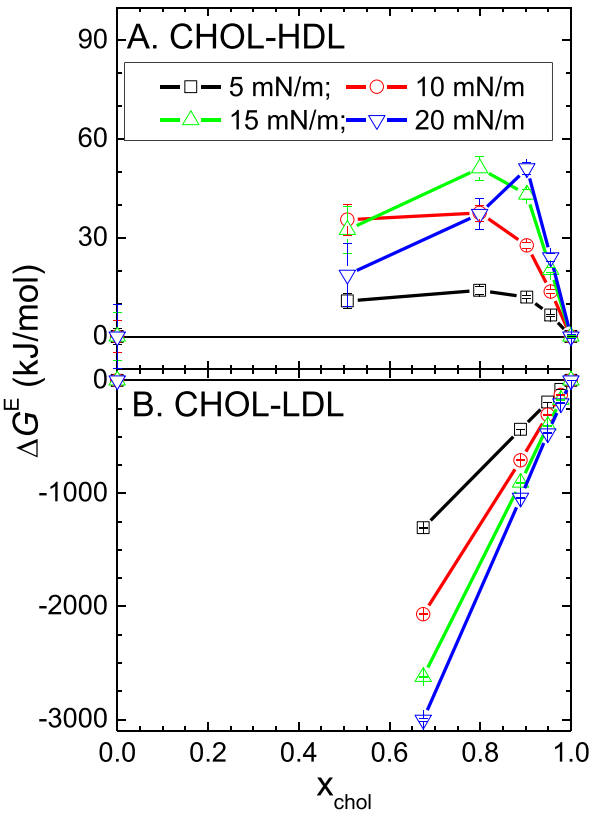

Figure 9. The excess free energy (ΔG^E) of Chol-HDL mixed monolayers (Panel A) and Chol-LDL mixed monolayers (panel B) as a function of the molar fraction of cholesterol (X_{Chol}) in the mixed monolayers for different surface pressures (∏).

The ΔG^M of the Chol-HDL or Chol-LDL mixed monolayers as a function of X_{Chol} is shown in Figure 10 for various surface pressures. A negative ΔG^M illustrates miscibility in the mixed monolayer and the presence of attractive interactions between the components of the mixed monolayer. Positive ΔG^M values indicate that the mutual interactions between the components are weaker than the interactions between the pure components themselves [41].

The values of ΔG^M were very similar to the ΔG^E values, regardless of the surface pressure, X_{Chol}, and the lipoprotein type. The values of ΔG^{id} for the Chol-HDL mixed monolayers and the Chol-LDL mixed monolayers (Table 3) were compared to the values shown in ΔG^E (Figure 9). Regardless of surface pressure and the lipoprotein type, ΔG^E was much greater than ΔG^{id}. Thus, the values of ΔG^M were concluded to be mostly determined by ΔG^E. The stability of the mixed monolayers are explained by ΔG^E, and therefore by the molecular interactions between the monolayer components in the mixed monolayers. The presence of attractions between cholesterol and the components in the LDL monolayer would explain why the Chol-LDL mixed monolayer is more stable than the Chol-HDL mixed monolayer.

4. Discussion

The size of the sterol domains increased as cholesterol was added to the pure HDL monolayer. This was explained by the onset of the phase separation of the sterol components from the non-sterol components of HDL. In contrast, the size of the sterol domains did not increase as much, if cholesterol was added to the LDL monolayer. The sterol molecules therefore did not appear to phase separate from the non-sterol components for the LDL case to the same extent as the HDL case. This difference is explained by a higher affinity between cholesterol and the non-sterol components (proteins and phospholipids) of LDL than that between cholesterol and the non-sterol components (proteins and phospholipids) of HDL. The thermodynamic analysis also suggested the presence of attractions between cholesterol and the components of LDL, while repulsions obviously appear to exist between cholesterol and the components of HDL.

As lipoprotein particles have been reported to break at the air/water interface and allow the liberation of the free lipids from the lipoprotein core [42], the air/water interface would be occupied by cholesterol molecules and the sterol, lipid and protein components of HDL and LDL in the case of the Chol-HDL mixed monolayers and the Chol-LDL mixed monolayers. The lipids found in LDL and HDL are similar [6,7]. However, the predominant apoprotein in HDL and LDL is different. Thus, the differences in the interaction of HDL and LDL with cholesterol are thought to be due to a difference in the interactions of the apoproteins of HDL and LDL with cholesterol.

The predominant apoprotein found in LDL and HDL is Apo-B and Apo-A, respectively. Apo-A is a soluble apoprotein, which contains amphiphilic α-helical repeat regions, where the charged amino groups are distributed on the hydrophilic regions [10]. Apo-B is a large hydrophobic protein that contains a large portion of β-sheet structure and only a small portion of amphiphilic α-helical structure [8,10]. These β-sheet regions are thought to be hydrophobic [10]. As cholesterol is an amphiphilic molecule, it may attach to the hydrophobic β-sheet areas of Apo-B via hydrophobic attractions. As Apo-A is less hydrophobic than Apo-B, it would not be able to interact with cholesterol via hydrophobic attractions as strongly as Apo-B. The stronger attractions between cholesterol and Apo-B compared to that between cholesterol and Apo-A would allow the cholesterol molecules to pack closer and more efficiently with Apo-B

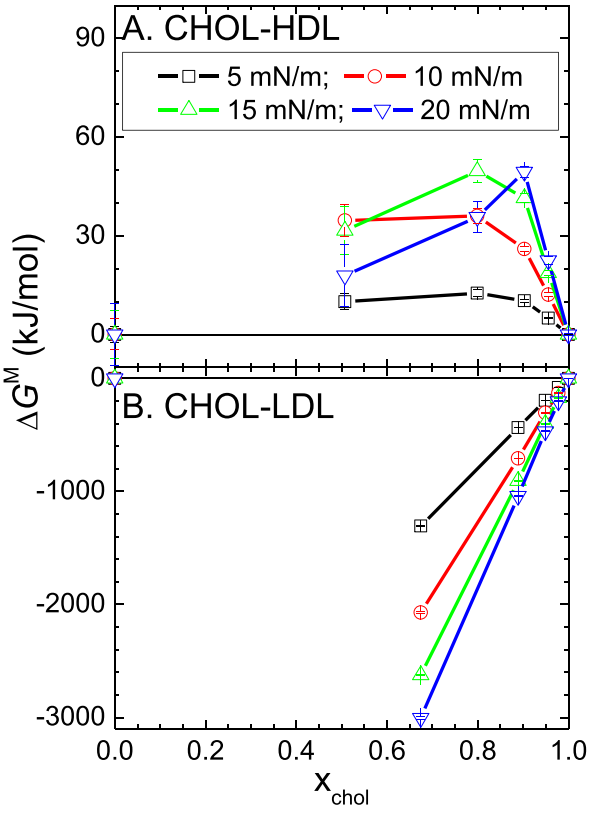

Figure 10. The Gibbs free energy of mixing (ΔG^M) of Chol-HDL mixed monolayers (Panel A) and Chol-LDL mixed monolayers (panel B) as a function of the molar fraction of cholesterol (X_{Chol}) in the mixed monolayers for different surface pressures (∏).

Table 3. The values of ΔG^{id} for the Chol-HDL mixed monolayer with different molar fractions of cholesterol (X_{Chol}).

Mixed monolayers	X_{Chol}	ΔG^{id} (kJmol^{-1})
Chol-HDL	0.96 ± 0.01	-0.8
	0.90 ± 0.01	-1.5
	0.80 ± 0.01	-1.7
	0.51 ± 0.01	-1.5
Chol-LDL	0.98 ± 0.01	-1.6
	0.95 ± 0.01	-0.9
	0.89 ± 0.01	-0.5
	0.67 ± 0.01	-0.3

than with Apo-A. The attractions would allow the steric repulsions caused by the inefficient packing of the cholesterol molecules with the non-sterol components of LDL to be partially overcome. The cholesterol domains formed in the Chol-HDL case would be larger than those seen in the Chol-LDL case, due to the absence or lower magnitude of these attractions. The cholesterol molecules would aggregate and phase separate from the non-sterol components of HDL, so as to reduce the steric repulsions in the system. Apo-B has previously been reported to interact favourably with cholesterol and its esters, particularly those between the hydrophobic amino acids of Apo-B and the ring of cholesterol esters, which have a structure similar to cholesterol [43]. There are also reports suggesting that cholesterol is partially excluded from the boundary region adjacent to Apolioprotein A-I, when the fraction of cholesterol in a system of phospholipid and Apolioprotein A-I is high enough [44]. Cholesterol therefore appears to interact with Apo-B better than with Apo-A. The hydrophobic attractions between Apo-B and cholesterol can be thought to help decrease the phase separation of the sterol molecules from the non-sterol components for the LDL case.

The favourable interaction of cholesterol with the apoproteins in an LDL particle can also be surmised from the structure of the LDL particle. An LDL particle is composed of a spherical bilayer of phospholipids, which is covered by proteins (main apoprotein is Apo-B). Free cholesterol and cholesteryl esters are found over each side of the bilayer. Each surface protein subunit is also associated with several cholesteryl esters [45]. The fact that the sterol molecules are found in the vicinity of the proteins suggests a favorable interaction between cholesterol and the Apo-B protein. Similarly, the less favourable interaction of cholesterol with the apoproteins in an HDL particle can be surmised from the structure of the HDL particle. The surface of a HDL particle is composed of apoproteins (main apoprotein is Apo-A) and other proteins, phospholipids, and steroids (e.g. free cholesterol). The core of the HDL particle is comprised of cholesteryl esters and triglycerides [46]. HDL is reported to collect cholesterol and carry it into its hydrophobic core, after converting cholesterol to the more hydrophobic, esterified form of cholesteryl ester via LCAT-mediated esterification [47]. The size of HDL spheres increase as more cholesterol is incorporated into the HDL core [48]. The fact that the sterol molecules are predominately carried in the core of the HDL particles away from the Apo-A protein suggests that the interaction between cholesterol and the Apo-A protein is less favorable than the interaction of cholesterol with components in the bulk of the HDL particle.

5. Conclusions

The addition of cholesterol to LDL or HDL monolayers to form Chol-LDL mixed monolayer and Chol-HDL mixed monolayers caused the Chol-LDL mixed monolayers to form sterol domains that were smaller in size but larger in number than those found in the Chol-HDL mixed monolayers. The thermodynamic analysis of the surface pressure-area per molecule isotherms of these monolayers suggested that the addition of cholesterol to HDL monolayers tended to cause partial phase separation in the Chol-HDL mixed monolayer. Such a phase separation onset was not observed to the same extent in the Chol-LDL mixed monolayer. Cholesterol was therefore concluded to show an improved interaction with LDL than with HDL. The improved interaction of cholesterol with LDL suggested an improved interaction between cholesterol and the apoproteins of LDL (Apo-B) rather than the interactions between cholesterol and the apoproteins of HDL (Apo-A). This finding is supported by the results of previous studies that show that Apo-B interacts favourably with cholesterol [39], but that cholesterol is partially excluded from the region adjacent to Apo-A [42]. We explained this improved interaction by the stronger hydrophobic attractions between cholesterol and Apo-B than that between cholesterol and Apo-A. The findings of our study suggest that if the interactions between cholesterol and the lipoprotein can be changed, then it may be possible to interact with the transport of cholesterol by lipoproteins.

Declarations

Author contribution statement

Cathy McNamee: Conceived and designed the experiments; Performed the experiments; Analyzed and interpreted the data; Contributed reagents, materials, analysis tools or data; Wrote the paper.

Ryota Ninomiya: Conceived and designed the experiments; Performed the experiments; Analyzed and interpreted the data; Contributed reagents, materials, analysis tools or data.

Funding statement

Cathy McNamee was supported by Shinshu University through the Promotion of Research by Young Scientists.

Competing interest statement

The authors declare no conflict of interest.

Additional information

No additional information is available for this paper.

References

[1] E. Ikonen, Cellular cholesterol trafficking and compartmentalization, Nat. Rev. Mol. Cell Biol. 9 (2008) 125–138.
[2] I. Hanukoglu, Steroidogenic enzymes: structure, function, and role in regulation of steroid hormone biosynthesis, Steroid Biochem. Mol. Biol. 43 (1992) 779–804.
[3] D.E. Vance, J.E. Vance, Biochemistry of Lipids, Lipoproteins and Membrane, Elsevier, Amsterdam, 2008, p. 486.
[4] P. Laggner, P. Laggner, in: G. Kostner (Ed.), Lipoproteins - Role in Health and Diseases, InTech, 2012.
[5] D.E. Vance, J.E. Vance, Biochemistry of Lipids, Lipoproteins and Membrane, Elsevier, Amsterdam, 2008, p. 487.
[6] L. Lagrost, L. Perségol, C. Lallemant, P. Gambert, Influence of Apoliprotein composition of high density lipoprotein particles on cholesterol ester transfer protein activity, J. Biol. Chem. 269 (1994) 3189–3197.
[7] J.D. Morrisett, R.L. Jackson, M. Gotto, Lipid-Protein interactions in the plasma lipoproteins, Biochim. Biophys. Acta 472 (1977) 93–133.
[8] M. Shaw, Lipoproteins as Carriers of Pharmacological Agents, Marcel Dekker Inc., New York, 1991, p. 3.
[9] D.E. Vance, J.E. Vance, Biochemistry of Lipids, Lipoproteins and Membrane, Elsevier, Amsterdam, 2008, p. 491.
[10] L. Chan, The apolipoprotein multigene family: structure, expression, evolution, and molecular genetics, Klin. Wochenschr. 67 (1989) 225–237.
[11] M. Taha Jalali, A. Mosavi Honomaror, A. Rekabi, M. Latifi, Reference Ranges for Serum Total Cholesterol, HDL-Cholesterol, LDL-Cholesterol, and VLDL-Cholesterol and Triglycerides in Healthy Iranian Ahvaz Population. Ind. J. Clin. Biochem. 28 (2013) 277–282.
[12] S. Dauphas, V. Beaumal, P. Gunning, A. Mackie, P. Wilde, V. Vié, A. Riaublanc, M. Anton, Structure modification in hen egg yolk low density lipoproteins layers between 30 and 45 mN/m observed by AFM, Colloids Surf. B Biointerfaces 54 (2007) 241–248.
[13] S. Dauphas, V. Beaumal, P. Gunning, A. Mackie, P. Wilde, V. Vié, A. Riaublanc, M. Anton, Structural and rheological properties of hen egg yolk low density lipoproteins layers spread at the air-water interface at pH 3 and 7, Colloids Surf. B Biointerfaces 57 (2007) 124–133.
[14] C.E. McNamee, G.T. Barnes, I.R. Gentle, J.B. Peng, R. Steitz, R. Probert, Evaporation resistance of mixed monolayers of octadecanol and cholesterol, J. Colloid Interface Sci. 207 (1998) 258–263.
[15] B.L. Stottrup, A.H. Nguyen, E. Tüzel, Taking another look with fluorescence microscopy: image processing techniques in Langmuir monolayers for the twenty-first century, Biochim. Biophys. Acta 1798 (2010) 1289–1300.
[16] G.T. Barnes, I.R. Gentle, Interfacial Science an Introduction, Oxford University Press, Oxford, 2005, p. 86.
[17] H. Ngyugen, C.E. McNamee, Determination and comparison of how the chain number and chain length of a lipid affects its interactions with a phospolipid at an air/water interface, J. Phys. Chem. B 118 (2014) 5901–5912.
[18] M. Savva, S. Acheampong, The interaction energies of cholesterol and 1,2-dioleoyl-sn-glycero-3-phosphoethanolamine in spread mixed monolayers at the air-water interface, J. Phys. Chem. B 113 (2009) 9811–9820.
[19] E. Guzmán, L. Liggieri, E. Santini, M. Ferrari, F. Ravera, Mixed DPPC-cholesterol Langmuir monolayers in presence of hydrophilic silica nanoparticles, Colloids Surf. B Biointerfaces 105 (2013) 284–293.
[20] R. Mallol, M.A. Rodríguez, M. Heras, M. Vinaixa, N. Plana, L. Masana, G.A. Morris, X. Correig, Particle size measurement of lipoprotein fractions using diffusion-ordered NMR spectroscopy, Anal. Bioanal. Chem. 402 (2012) 2407–2415.
[21] V.B. Kamat, G.A. Lawrence, M.D. Barratt, A. Darke, R.B. Leslie, G.G. Skipley, J.M. Stubbs, Physical Studies of egg yolk low density lipoprotein, Chem. Phys. Lipids 9 (1972) 1–25.
[22] V. Martinet, P. Saulnier, V. Beaumal, J.-L. Courthaudon, M. Anton, Surface properties of hen egg yolk low-density lipoproteins spread at the air-water interface, Colloids Surf. B Biointerfaces 31 (2003) 185–194.
[23] P. Jolivet, C.I. Boulard, T. Chardot, M. Anton, New insights into the structure of apolipoprotein B from low-density lipoproteins and identification of a novel YGP-like protein in hen egg yolk, J. Agric. Food Chem. 56 (2008) 5871–5879.
[24] J. Yang, Y. Li, E. Liu, T.W. Xininigen, W. Bai, R. Han, Using rifapentine – hen egg lipoprotein as macrophage-targeted drug delivery carrier against intracellular Staphylococcus aures, Drug Deliv. 22 (2015) 111–116.
[25] C.A.S. Andrade, N.S. Santos-Magalhães, C.P. de Melo, Thermodynamic characterization of the prevailing molecular interactions in mixed floating monolayers of phospholipids and usnic acid, J. Colloid Interface Sci. 298 (2006) 145–153.
[26] G.L. Gains, Insoluble Monolayers at Liquid-Gas Interfaces, Interscience Publishers, New york, 1966, p. 24.
[27] H. Zhu, R. Sun, C. Hao, P. Zhang, A Langmuir and AFM study on interfacial behaviour of binary monolayer of hexadecanol/DPPE at the air-water interface, Chem. Phys. Lipids 201 (2016) 11–20.
[28] J. Smaby, V.S. Kulkarni, M. Momsen, R.E. Brown, The interfacial elastic packing interactions of galactosylceramides, sphingomyelins, and phosphatidylcholines, Biophys. J. 70 (1996) 868–877.
[29] J. Wang, R. Sun, Influence of alkane phosphatase on phase state of the SM monolayers at the air-water interface, Colloid Surf. A-Physicochem. Eng. 489 (2016) 136–141.
[30] J.T. Davies, E.K. Rideal, Interfacial Phenomena, Academic Press, New York, 1963, p. 265.
[31] A.E. Anwander, R.P.J.S. Grant, T.M. Letcher, Interfacial phenomena, Chem. Educ. 65 (1988) 608–614.
[32] I. Rey Gómez-Serranillos, J. Miñones Jr., P. Dynarowicz-Łątka, J. Miñones, E. Iribarnegaray, Miltefosine-cholesterol interactions: a monolayer study, Langmuir 20 (2004) 928–933.
[33] E. Guzmán, L. Liggieri, E. Santini, M. Ferrari, F. Ravera, Mixed DPPC-cholesterol Langmuir monolayers in presence of hydrophilic silica, Colloids Surf. B Biointerfaces 105 (2013) 284–293.
[34] J.L. Fidalgo Rodriguez, L. Caseli, J. Minones Conde, P. Dynarowicz-Łątka, New look for an old molecule – solid/solid phase transition in cholesterol monolayers, Chem. Phys. Lipids 225 (2019) 104819.
[35] A. Wnętrzak, E. Lipiec, K. Łątka, W. Kwiatek, P. Dynarowicz-Łątka, Affinity of alkylphosphocholines to biological membrane of prostate cancer: studies in natural and model systems, J. Membr. Biol. 247 (2014) 581–589.
[36] B. Krajewska, A. Kysioł, P. Wydro, Chitosan as a subphase disturbant of membrane lipid monolayers. The effect of temperature at varying pH: II. DPPC and cholesterol, Colloid Surf. A-Physicochem. Eng. 434 (2013) 359–364.
[37] R. Seoane, J. Miñones, O. Conde, J. Miñones, M. Casas, E.J. Iribarnegaray, Thermodynamic and Brewster angle microscopy studies of fatty acid/cholesterol mixtures at the air/water interface, J. Phys. Chem. B 104 (2000) 7735–7744.
[38] G.L. Gains, Insoluble Monolayers at Liquid-Gas Interfaces, Interscience Publishers, New york, 1966, pp. 291–292.
[39] B. Gzyl-Malcher, M. Paluch, Studies of lipid interactions in mixed Langmuir monolayers, Thin Solid Films 516 (2008) 8865–8872.
[40] G. He, R. Sun, C. Hao, J. Yang, M. Wang, L. Zhang, Thermodynamic analysis and AFM study of the interaction of palmitic acid with DPPE in Langmuir monolayers, Colloid Surf. A-Physicochem. Eng. 441 (2014) 184–194.
[41] R. Maget-Dana, The monolayer technique: a potent tool for studying the interfacial properties of antimicrobial and membrane-lytic peptides and their interactions with lipid membranes, Biochim. Biophys. Acta-Biomembr. 1462 (1999) 109–140.
[42] B. Lemkadem, F. Boury, P. Saulnier, J.E. Proust, Interfacial behavior of HDL3 spread at air/water interface. I. Dynamic Properties, Colloids Surf. B Biointerfaces 13 (1999) 221–231.
[43] T. Murtola, T.A. Vuorela, M.T. Hyvönen, S. Marrink, M. Karttunen, I. Vattulainen, Low density lipoprotein: structure, dynamics, and interactions of aopB-100 with lipids, Soft Matter 7 (2011) 8135–8141.
[44] B.B. Lundberg, Incorporation of cholesterol into apolipoprotein A-I-dimydristoylphosphatidylcholine recombinants, Biochim. Biophys. Acta 962 (1988) 265–274.
[45] C.E. Day, R.S. Levy, Low Density Lipoproteins, Plenum Press, New York, 1976, p. 33.
[46] A. Kontush, M.J. Chapman, High-density Lipoproteins Structure, Metabolism, Function and Therapeutics, John Wiley & Sons, New Jersey, 2012, pp. 3–38.
[47] A. Kontush, M.J. Chapman, High-density Lipoproteins Structure, Metabolism, Function and Therapeutics, John Wiley & Sons, New Jersey, 2012, pp. 86–87.
[48] A. Kontush, M.J. Chapman, High-density Lipoproteins Structure, Metabolism, Function and Therapeutics, John Wiley & Sons, New Jersey, 2012, p. 887.